General Role of GDP Dissociation Inhibitor 2 in Membrane Release of Rab Proteins: Modulations of Its Functional Interactions by in Vitro and in Vivo Structural Modifications†

Assia Shisheva,* Sreenivasa R. Chinni, and Carmen DeMarco

Department of Physiology, Wayne State University School of Medicine, 540 East Canfield Street, Detroit, Michigan 48201

Received January 27, 1999; Revised Manuscript Received June 4, 1999

ABSTRACT: The GDP dissociation inhibitors (GDIs) represent an important class of regulatory proteins in the functional cycle and recycling of Rab GTPases. Previous studies have demonstrated that GDI-1 can operate with multiple Rab proteins. In this study we have addressed a plausible general activity of GDI-2 in supporting Rab membrane release and have analyzed the requirements of sequence-conserved vs variable regions of GDI-2 in these functional interactions. The in vitro function of expressed recombinant GDI-2 wild-type-, point-, or deletion-mutant proteins was investigated toward several Rab family members, divergent in structure, localized and operating on different membranes, including Rab2, Rab4, Rab5, Rab8, Rab9, and Rab11. We demonstrate here a general and nearly invariant ability of GDI-2^{WT} to release from membranes this subset of diverse Rabs. Deletion of an 18-residue segment from the C-terminal variable region yielded a fully functional or only slightly defective GDI-2. Conversely, substitution of Met at position 250 of the conserved region markedly abrogated the activity toward all Rabs. Surprisingly, a replacement of an adjacent conserved residue (Y249V) resulted in a selective Rab-dependent response and a profound gain of function toward specific Rabs. To further test whether the endogenous GDI-2 can adopt a gain-of-function conformation, we pharmacologically stimulated intact 3T3-L1 adipocytes to induce GDI-2 tyrosine phosphorylation. We found a pronounced increase of the Rab4 soluble form and its soluble complexes with the tyrosine-phosphorylated GDI-2. Together, these results indicate that (a) GDI-2 displays a general activity to release Rabs from membranes, (b) GDI-2-conserved residues, but not the C-terminal variable region, are essential for this activity, and (c) structural modifications in GDI-2 can enhance its functional activity, directing selective interactions with individual Rabs.

Accumulated evidence over the past several years points to a functional role for the Rab/YPT1/SEC4 gene subfamily of p21 ras-like small GTP-binding proteins in the mechanisms regulating membrane trafficking in yeast and mammalian cells (for recent reviews, see refs *1*−*4*). Reported data are consistent with the notion that Rabs are essential in each step of vesicular transport, including vesicle formation, vesicle docking, and membrane fusion (*4*). We possess limited knowledge about the specific function and molecular mechanism(s) of action for each individual Rab protein (more than 40 presently known members). It is largely accepted that the distinct compartment specificity, a hallmark of the mammalian Rabs, predicts the transport step they regulate. Current models suggest that Rab GTPases cycle between a cytosolic, inactive, GDP-bound state, and a membrane-bound, active, GTP-bound state. When the cytosolic form of Rabs is recruited to the cytoplasmic leaflet of the donor organelle, it is activated by the exchange of GDP for GTP. Once on a carrier vesicle, activated Rabs regulate docking and fusion by interacting with yet to be defined specific elements of the membrane transport machinery (*1*−*4*). Studies in yeast imply a role of Rabs in dissociating an inhibitory protein that impairs vSNARE and tSNARE recognition, allowing their assembly (*5*, *6*). GTP hydrolysis is probably not conditional on membrane fusion but rather acts as a timer determining the frequency of docking/fusion events (*7*). After fusion has occurred, Rabs are solubilized by GDP dissociation inhibitors (GDIs),[1] a ubiquitous family of highly related proteins, which escort them back to the donor membrane, completing the cycle and allowing its multiple rounds (*8*).

Among the three presently known members of the GDI protein class (GDI-1, also known as RabGDI or GDIα, GDI-2, and GDIβ; refs *9*−*13*), GDI-1, the best-studied member, appears crucial for progression through the membrane/cytosol localization cycle and the recycling of all Rabs studied thus far. In line with this requirement are the reported numerous properties of GDI-1: formation of stable cytosolic complexes with GDP-loaded prenylated Rabs (*14*−*16*); presentation of functional Rabs to membranes contributing in the specific recognition of the Rab membrane targets (*15*−*17*); stimula-

* Address correspondence to this author at the Department of Physiology, Wayne State University School of Medicine, 540 E. Canfield St., Detroit, MI 48201. Telephone: (313) 577-5674. FAX: (313) 577-5494. E-mail: ashishev@moose.med.wayne.edu.

† This project was supported by American Diabetes Association Career Development Award (A.S.) and by Juvenile Diabetes Foundation International Research Grant 196114 (A.S.). Part of this study was presented at the 38th American Society for Cell Biology Annual Meeting, San Francisco, CA, Dec 13−16, 1998.

[1] Abbreviations: GDI, GDP dissociation inhibitor isoform; DMEM, Dulbecco's modified Eagle's medium; FBS, fetal bovine serum; PBS, phosphate-buffered saline; GST, glutathione *S*-transferase; PMSF, phenylmethanesulfonylfluoride; PAGE, polyacrylamide gel electrophoresis; PCR, polymerase chain reaction; anti-PY, anti-phosphotyrosine; SCR, sequence-conserved region.

10.1021/bi990200r CCC: $18.00
Published on Web 08/17/1999

tion of Rab GDP/GTP exchange factor (*18*); its own dissociation back into the cytosol, likely promoted by GDI dissociation factor(s) (*19*) and/or a redox-dependent mechanism (*20*); and, finally, retrieval of "spent" Rab proteins for returning them back to their membrane of origin (*14*). It still remains to be determined whether this whole array of different functions are shared by the other two members of the mammalian GDI protein class, GDI-2 and GDIβ. Because GDIs display a high degree of homology (86% and 96% identity between GDI-2 and GDI-1, or GDIβ, respectively), it is largely accepted, yet not proven, that they exhibit a redundant function. Although several lines of biochemical and morphological evidence suggest distinct functional roles for GDI-1 and GDI-2 in the context of living cells (*21*−*23*), no specificity toward an individual Rab or a subset of Rab proteins has been documented thus far. Thus, in in vitro assays, the three GDIs display similar abilities to bind and solubilize membrane-associated Rab protein members in a GDP/GTP-dependent manner, although this has been directly demonstrated in a comparable fashion only for limited Rab members (*11*). Concordantly, when overexpressed to comparable levels in living cells, GDI-1 and GDI-2 display indistinguishable ability to solubilize individual Rabs (*24*). Conceivably, in the context of intact cells, a given Rab can form cytosolic complexes simultaneously with all three GDI isoforms (*23*, *25*).

Structural studies of GDI-1 combined with site-directed mutagenesis demonstrated that two sequence-conserved regions (SCRs), designated as 1 and 3B, common to GDIs and to a closely related family of proteins supporting Rab prenylation (the choriodermia gene products REP1 and REP2), fold to form a plausible Rab-binding region at the apex of the molecule (*26*). Several amino acids of the GDI-1 molecule, including Y^{39}, E^{233}, T^{248}, Y^{249}, and M^{250}, are shown critical in Rab interaction (*26*). While extensive structure−function information has been obtained for GDI-1, virtually nothing is known about the region of GDI-2 involved in Rab interaction. As a first step toward understanding a plausible GDI-2 general activity in the Rab cycle and identification of key functional domains and residues, we generated recombinant GDI-2 molecules that were truncated at the highly variable carboxyl termini, or point-mutated at predicted key Rab-binding amino acids in the sequence-conserved region 3B. Purified proteins were analyzed in functional interactions with a diverse group of Rab proteins, including Rab2, Rab4, Rab5, Rab8, Rab9, and Rab11. We demonstrate here that GDI-2 can solubilize all of them with similar efficacies. While a GDI-2 C-terminal deletion of 18 amino acids does not significantly affect Rab retrieval, a point mutation at position 250 dramatically abrogates the functional interactions with Rabs. Surprisingly, while GDI-2^{WT} indiscriminately retrieves all of the membrane Rabs examined here, the substitution of Tyr^{249} results in profound differential effects and a marked gain-of-function with particular Rabs. We provide further experimental evidence suggesting that GDI-2 tyrosine phosphorylation in living cells can selectively modify its functional interaction with individual Rab proteins.

MATERIALS AND METHODS

Materials. Renaissance chemiluminescence detection kit and ^{125}I−protein A were purchased from New England Nuclear (Boston, MA); glutathione−agarose beads were from Sigma (St. Louis, MO); nitrocellulose or Immobilon P transfer membranes (0.45 μm pore size) were from Schleicher & Schuell (Keene, NH) and Millipore Corp. (Bedford, MA); protein assay reagents were from BioRad (Hercules, CA) or Pierce (Rockford, IL); horseradish peroxidase-coupled anti-rabbit IgG and horseradish peroxidase-coupled anti-mouse IgG were from Boehringer Mannheim Corp. (Indianapolis, IN). Monoclonal anti-PY antibody (4G10) was from UBI (Lake Placid, NY). Monoclonal antibodies against Rab5 and Rab9 were gifts from M. Zerial and S. Pfeffer. Polyclonal antibodies against Rab2, Rab4 (R10502), Rab8, and Rab11 were gifts from M. Zerial and I. Mellman. Anti-GDI-2 (R3361 and R3362) and anti-GDI-1 (R3357) antisera, characterized previously (*11*, *21*), were utilized as IgG fractions purified on protein A−Sepharose columns. Peroxides of vanadate (pervanadate) were prepared by mixing sodium metavanadate (40 mM) with H_2O_2 in a 1:2 molar ratio for 15 min at 22 °C as we previously described (*27*).

Cell Cultures. 3T3-L1 mouse fibroblasts, grown to confluence (150 mm plate) in DMEM containing 10% calf serum, 50 units/mL penicillin, and 50 μg/mL streptomycin sulfate, were differentiated into adipocytes as previously described (*11*). Adipocytes were used between days 8 and 12 after the onset of differentiation. COS-7 cells were grown to the indicated density (150 mm plate) in DMEM containing 10% FBS and the above antibiotics.

Generation of GDI-2 Point and Deletion Mutants. The *Eco*RI fragment of pBluescript-mGDI-2 cDNA, consisting of the entire coding region of mouse GDI-2 (*11*), was subcloned into an *Eco*RI digest of pGEM-easy vector (Promega) to avoid the *Kpn*I and *Eco*RV restriction sites in the polylinker. Point mutants of GDI-2 were constructed by PCR combined with restriction digest. Specifically, to generate mGDI-2^{Y249V} cDNA, a standard PCR protocol was performed using pBluescript-mGDI-2 cDNA (*11*) as a template, and sense and antisense primers spanning nucleotides 735−760 (5′-TGGAGGTACCGTGATGCTGAA TAAAC, changed triplet is underlined) and nucleotides 1062−1045 (5′-GCTGGCAATGGCGATGT), respectively, of the GDI-2 nucleotide sequence (*11*). The amplified PCR product (327 bp) was isolated and digested with *Kpn*I and *Eco*RV to release a 250 bp oligonucleotide, which was then subcloned into the *Kpn*I−*Eco*RV sites of pGEM-easy-mGDI-2 cDNA. The cDNA of the mGDI-2^{M250Y} point mutant was constructed using principally the same strategy except for a sense primer (5′-GGAGGTACCTACTACCTGAAT-AAACCAAT, changed triplet is underlined). PCR products corresponding to each mutant were sequenced with the antisense primer to confirm the sequence and the desired mutations. A C-terminal deletion mutant, GDI-$2^{\Delta C18}$, was generated by digesting the pCMV5-mGDI-2 cDNA with *Bam*H, which eliminated a 54-nucleotide fragment from the C-terminus of the GDI-2 coding region.

Production of GST−GDI-2 Fusion Proteins. The entire mGDI-2 protein was expressed as a GST fusion protein in pGEX-1 vector (Amrad) as described elsewhere (*11*). GDI-2^{Y249V} and GDI-2^{M250Y} cDNAs constructed as described above were cloned into the *Eco*RI site of pGEX-1 in-frame with the GST gene. The *Eco*RI−*Sma*I fragment of the C-terminal deletion mutant pCMV5-GDI-$2^{\Delta C18}$ was subcloned into the *Eco*RI−*Sma*I digest of pGEX4T-1 (Pharmacia). The proper organization of the constructs was

confirmed by restriction mapping. *E. coli* XA-90 strain was used for transformations. Transformed cells were grown and treated with 0.5 mM isopropyl-1-thio-β-D-galactopyranoside for 4 h. The cells were collected, resuspended in a buffer (50 mM Hepes, pH 7.4, 150 mM NaCl, 5 mM EDTA, 1% Triton X-100, 1 mM PMSF, 1 mg/mL benzamidine, 5 μg/mL aprotinin, and 5 μg/mL leupeptin), and lysed with lysozyme (1 mg/mL) at 4 °C. Following several rounds of freezing and thawing, the lysates were sonicated for 1 min and centrifuged at 12000*g* for 25 min at 4 °C. The supernatant was applied to glutathione−agarose beads that were extensively washed with 50 mM Tris-HCl, pH 8.0, containing 0.05% Triton X-100. GST−GDI-2 wild-type or mutant fusion proteins were eluted with the same buffer, containing 5 mM glutathione, which was removed thereafter by repeating ultrafiltration in a Centricon 30 microconcentration unit (Amicon). The concentrations and quality of the purified proteins were determined electrophoretically by the intensity of the Coomassie blue-stained protein bands relative to BSA standards (Figure 1).

Cell Treatment. Prior to experiments, 3T3-L1 adipocytes were serum-starved for 3 h in DMEM and then treated with pervanadate (100 μM) or insulin (100 nM) in DMEM for 20 min at 37 °C. The cells were then washed with PBS at room temperature. The cells were then scraped and homogenized at 4 °C in the "homogenization buffer" (20 mM Hepes, pH 7.4, 255 mM sucrose, 1 mM EDTA), supplemented with 5 mM $MgCl_2$, 1 mM GDP, 1 × phosphatase inhibitor mixture (25 mM β-glycerophosphate, 100 mM NaF, 2 mM sodium orthovanadate), and 1 × protease inhibitor mixture (1 mM PMSF, 0.5 mg/mL benzamidine, 5 μg/mL leupeptin, 5 μg/mL aprotinin, and 1 μg/mL pepstatin). The cytosolic fractions were then obtained by centrifuging 17000*g* supernatants for 24 min at 200000*g* in a Beckman TLA 100.3 rotor. Equal amounts of protein (typically between 1 and 1.5 mg; determined by bicinchoninic acid protein assay) were immunoprecipitated with anti-Rab4, or with preimmune IgG cross-linked to protein A Sepharose Fast Flow.

In Vitro Dissociation Assay. COS-7 cells (serum-starved for 5 h before the experiment) were washed twice prior to homogenization at 4 °C in the "homogenization buffer", supplemented with 1 × protease inhibitor mixture. Postnuclear membrane fraction was obtained after two consecutive centrifugations: 10 min at 800*g*, and 15 min at 200000*g* (Beckman TL-100 Ultracentrifuge). Equal amounts (typically 100 μg of membrane protein) were incubated for 30 min at 30 °C in the presence of either GST-GDI-2^{WT}, mutant fusion proteins, or GST alone at concentrations indicated in the figure legends in a reaction buffer consisting of 50 mM Hepes/KOH, pH 7.6, 5 mM $MgCl_2$, 1 mM DTT, and supplemented with 1 × protease inhibitor mixture. Where indicated, prior to the above-described incubation, the membranes were pretreated for 45 min at 30 °C with GTPγS or GDP (each 1 mM). The reaction mixtures were pelleted (10 min, 200000*g*), and the membranes and the soluble fractions were analyzed for Rab2, Rab4, Rab5, Rab8, Rab9, and Rab11 contents by SDS−PAGE and immunoblotting with the corresponding antibodies.

Immunoprecipitation and Western Blotting. Rab4 immunoprecipitation was achieved on anti-Rab antibody cross-linked to Protein A Fast Flow as we described previously (*23*). Coupled IgG fractions equivalent to 14 of μL packed beads (~50 μg of IgG) were incubated with fractionated 3T3-L1 adipocyte cytosols in the presence of 1 mM GDP for 40 min at 4 °C. The beads were then quickly washed twice with 1.4 mL portions of "cytosol washing buffer", consisting of 20 mM Tris/HCl, pH 7.5, 0.1% Triton X-100, 2 mM EDTA, 25 mM NaCl, 5 mM $MgCl_2$, 0.8 mM GDP, 25 mM β-glycerophosphate, 25 mM NaF, 2 mM sodium orthovanadate, and 1 × protease inhibitor mixture by spinning down for 30 s at 10 000 rpm at 4 °C each time. The beads were then eluted stepwise as we previously described (*23*). Briefly, Rab4-associated proteins were first eluted for 20 min at 37 °C with 50 μL of RIPA buffer (20 mM Tris/HCl, pH 7.5, containing 1.2% Triton X-100, 0.5% sodium deoxycholate, 0.1% SDS, 2 mM EDTA, 132 mM NaCl, 5 mM $MgCl_2$, and the above phosphatase and protease inhibitors). Following centrifugation, 40 μL aliquots were decanted, reduced with Laemmli sample buffer (*28*), and analyzed by SDS−PAGE and Western blotting with anti-GDI-2 or anti-PY antibodies. In the second step, Rab4 was dissociated from the immunoaffinity columns by boiling in Laemmli sample buffer, and, following protein resolution by SDS−PAGE, was detected by Western blotting with anti-Rab4 antiserum. In some experiments, GDI-2 was immunoprecipitated from lysates of 3T3-L1 adipocytes using anti-GDI-2 antiserum (R3362; ref *21*). The immunoprecipitates were washed with RIPA buffer, reduced in Laemmli sample buffer, and, after SDS−PAGE, detected by immunoblotting with anti-GDI-2 and anti-PY antibodies.

For Western blotting, aliquots of the samples (15−70 μg of protein) were analyzed by SDS−PAGE under reducing conditions (*28*). Following electrophoretic separation, the proteins were electro-transferred to a nitrocellulose membrane. Membranes were blocked by incubation with 3% nonfat dry milk and 2% BSA or only 2% BSA (for 4G10 antibody) in 30 mM Tris, pH 7.4, 150 mM NaCl, 0.05% Tween 20 ("wash buffer"). The blots were incubated for 16 h at 4 °C with the antibodies indicated in the figure legends. Blots were then washed 5 times with "wash buffer" for 15 min each time. Bound antibodies were detected with horseradish peroxidase-bound anti-rabbit or anti-mouse IgG and chemiluminescence as indicated in the figure legends. In some experiments, bound antibodies were detected with ^{125}I-protein A (1 h at 25 °C) and autoradiography.

Protein levels on the blots were quantified on a laser densitometer (Molecular Dynamics) by area integration scanning. Several exposures of each blot were quantified to ensure that the chemiluminiscence exposures were within the linear range of the film. Additionally, immunoreactivity was quantified by cutting rectangular strips from ^{125}I-protein A-detected blots, corresponding to the band of interest, and analyzing their radioactivity on a Beckman 5500 γ-counting system. The between-assay variation coefficient for the in vitro dissociation assay calculated as described elsewhere (*29*) was 11.6%.

RESULTS

GDI-2 Solubilizes a Variety of Rabs with Similar Efficiency. Several laboratories including our own have shown that exogenously added GDI-1 is capable of solubilizing a

Table 1: Amino Acid Identities between the Indicated Rab Proteins[a]

	Rab2	Rab4	Rab5	Rab8	Rab9	Rab11
Rab2	100					
Rab4	56	100				
Rab5	39	41	100			
Rab8	46	43	40	100		
Rab9	38	38	39	40	100	
Rab11	54	48	41	42	38	100

[a] The table was produced by pairwise comparison of the human sequences by using the Basic Logic Alignment Search Tool (BLAST). The amino acid sequences used for the analyses are obtained from the following Swiss-Prot accession numbers: Rab2, P08886; Rab4A, P20338; Rab5B, P35239; Rab8, P24407; Rab9, P51151; Rab11A, P24410.

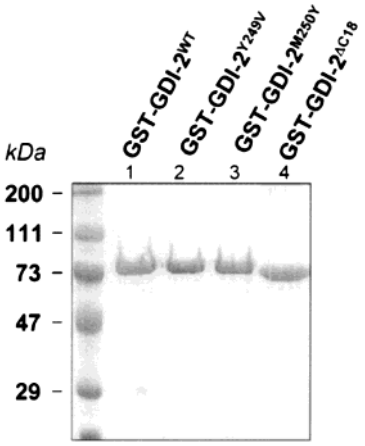

FIGURE 1: Purity of generated recombinant GST−GDI-2^{WT} or mutant proteins. Indicated mutants were generated by PCR combined with restriction digestion. The cDNAs of GDI-2^{WT}, GDI-2^{Y249V}, or GDI-2^{M250Y} were subcloned in pGEX-1, and that of GDI-$2^{\Delta C18}$, in pGEX4T-1. *E. coli* strain was transformed, and the GST-fusion proteins were produced and purified as described under Materials and Methods. Purified proteins were analyzed by SDS−PAGE as indicated. Coomassie blue-stained gels demonstrate highly pure products with practically no proteolyzed fragments in all four constructs.

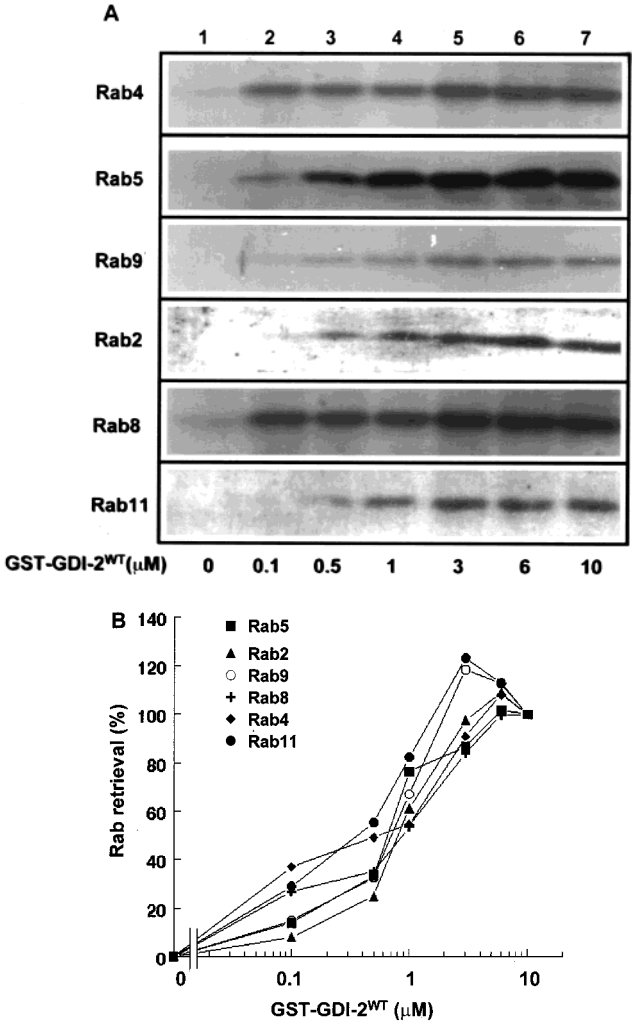

FIGURE 2: Effect of GST−GDI-2^{WT} in solubilizing membrane Rabs. Isolated COS-7 postnuclear membranes were preloaded with 1 mM GDP and were then incubated for 30 min at 30 °C in the presence of the indicated concentrations of GST−GDI-2^{WT} (0−10 μM). The reaction mixtures were centrifuged, and soluble fractions were analyzed by SDS−PAGE and immunoblotting with the indicated anti-Rab antibodies. (A) Chemiluminescence detections of representative immunoblots. (B) Quantification of their densitometric scans expressed as a percentage of the intensity at the highest GST−GDI-2^{WT} dose (10 μM) for each Rab, and plotted as a function of the GST−GDI-2^{WT} concentration. The standard error of the mean for three to four independent experiments for each individual Rab was <11% of the reported values.

wide range of membrane-bound Rab proteins. Intriguingly, GDI-1 performs this function with equal efficacy, despite the fact that individual Rabs are structurally distinct, and are localized on different membrane organelles in a context of a different intracellular membrane environment (*11*, *14*, *30*−*32*). With regard to GDI-2, available data provide limited information, and only three Rab family members, i.e., Rab1B, Rab4, and Rab5, have been studied thus far (*11*, *32*). To examine whether GDI-2, like GDI-1, operates with a diverse group of Rab proteins, we analyzed the functional ability of recombinant GDI-2 to extract several Rab species utilizing an in vitro assay with isolated COS-7 cell membranes (*11*). Paired comparison of Rab-deduced amino acid sequences demonstrated only a limited homology among them (Table 1). GDI-2 used in this study was produced as a GST fusion protein in bacterial hosts and was affinity-purified on glutathione−agarose beads to near-homogeneity as evident by the single protein band of 76 kDa detected on Coomassie blue-stained gels (Figure 1, lane 1). Increasing concentrations of the recombinant GDI-2 protein were incubated with isolated and washed COS membranes preloaded with GDP. Upon completion of the incubation, the levels of immunoreactive Rabs were detected in both the soluble and membrane fractions, following protein resolution by SDS−PAGE. Figure 2 shows an experiment in which we examined the ability of GST−GDI-2^{WT} to bind and solubilize GDP-loaded Rab2, Rab4, Rab5, Rab8, Rab9, and Rab11 from isolated COS membranes. In the absence of GST−GDI-2, no detectable levels of Rabs were documented in the soluble fraction (Figure 2A, lane 1). However, increasing amounts of added recombinant GDI-2 progressively increased the amounts of Rabs released into the soluble fraction (Figure 2A, lanes 2−7); this in turn was accompanied by proportionally decreasing the levels of membrane-bound Rab populations (data not shown). As expected, substitution of GDP for GTPγS largely inhibited this effect (see below). Densitometric scans of control immunoblots demonstrated a linear relationship between the amount of each one of the antigens analyzed here and the signal detected by chemiluminescence

Table 2: Half-Maximal Effective Concentration of GST−GDI-2^{WT} and Capacity of GST−GDI-2^{WT} To Retrieve Rabs[a]

	EC_{50} (μM)	GST−GDI-2^{WT} Rab retrieval capacity (% of total membrane levels)
Rab2	0.92	36
Rab4	1.00	27
Rab5	0.90	29
Rab8	0.91	31
Rab9	0.87	36
Rab11	0.66	38

[a] The EC50 values for different Rabs were calculated from the saturation curves presented in Figure 2B, by determining the concentration of GST−GDI-2^{WT} necessary to achieve 50% of its maximal effect. The capacity of GST GDI-2^{WT} to dissociate each individual Rab from membranes was estimated by comparing the portion of solubilized Rab vs its total membrane-associated levels. For this purpose, isolated COS-7 membranes were incubated or not incubated with GST−GDI-2^{WT} (1 μM) in the presence of GDP (1 mM) as described under Materials and Methods. Following incubation and centrifugation, the initial membrane fractions and the soluble fractions were analyzed by SDS−PAGE and immunoblotting with anti-Rab antibodies. Chemiluminescence-detected Rab protein bands were quantified by densitometric scanning. Values are expressed as a percentage of the total membrane-associated Rabs.

at relatively short exposed films (*23*, and data not shown). These results provide experimental evidence supporting the idea that GDI-2, like GDI-1 in similar assays, could recognize and dissociate various GDP-loaded Rabs, regardless of their structural variations, different intracellular membrane localization, and specific function.

To determine whether GDI-2 solubilizes different Rabs with equal efficacies, we analyzed the substrate saturation curves presented in Figure 2B. These analyses revealed that saturating concentrations of GDI-2 were similar for all Rabs examined, ranging from 3 to 4 μM. The half-maximal effective concentrations of GDI-2 (EC_{50}) were also found to be close for all Rabs, ranging between 0.66 and 1.0 μM (Figure 2 and Table 2). These data support the notion that a nonmodified/resting conformation of the recombinant GDI-2^{WT} protein does not significantly discriminate between the different Rabs but rather displays a general extraction phenotype for all Rab family members examined in this study.

Although saturation in the GDI-2^{WT} potency to extract Rabs from membranes has been established for each individual member as documented in Figure 2A, significant portions of Rabs remained membrane-associated under these conditions. Thus, at 1 μM concentration of GST−GDI-2^{WT}, the amounts of Rabs released into the soluble fraction amounted to only 27−38% of the total levels of membrane-associated Rabs (Table 2). This phenomenon has also been reported for a bacterially produced recombinant GDI-1 protein, which displays a partial Rab extraction even at saturating concentrations (*11*, *26*, *31*, *33*, *34*). Together these results are consistent with the notion that, under the conditions of the in vitro functional assays, recombinant GDIs are probably not fully active and suggest the possibility for posttranslational modifications in regulating their activity in living cells.

Carboxyl Terminus of GDI-2 Is Not Involved in Rab Membrane Release. As a first step toward determining key regions of GDI-2 responsible for its functional interactions with Rabs, a truncation of the C-terminal 18-residue segment

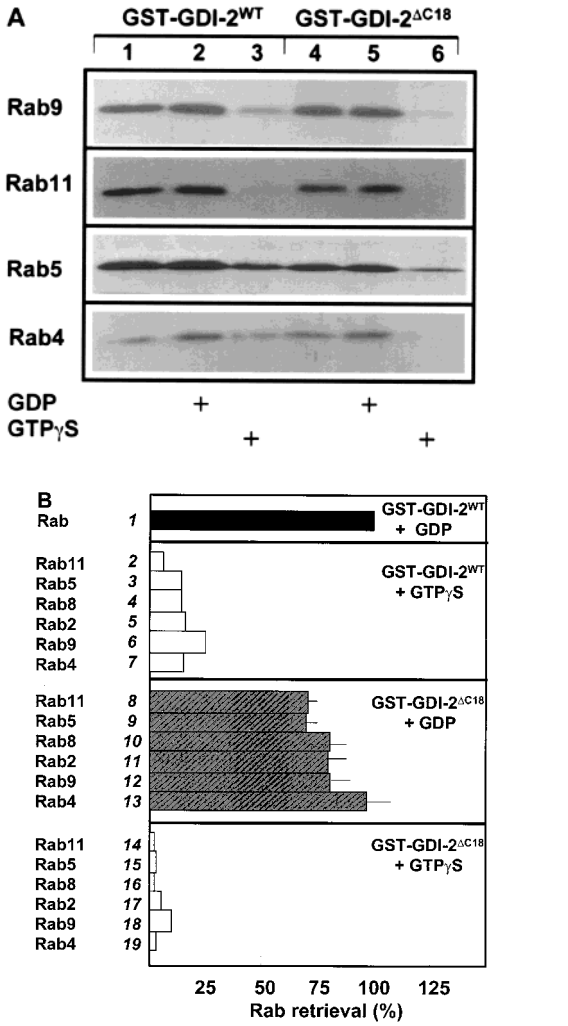

FIGURE 3: GST−GDI-$2^{\Delta C18}$ deletion mutant displays only slightly reduced GDI-2^{WT} activity in solubilizing Rabs. Postnuclear membranes isolated from COS-7 cells were preloaded with either GDP or GTPγS (each at 1 mM) for 45 min at 30 °C and were then incubated in the presence of GST−GDI-2^{WT} (1 μM) or GST−GDI-$2^{\Delta C18}$ (1 μM) for 30 min at 30 °C. The reaction mixtures were pelleted, and soluble fractions were analyzed by SDS−PAGE and immunoblotting with the indicated anti-Rab antibodies. Shown are chemiluminescence detections of representative immunoblots (A) and the quantification of densitometric scans (B) from three to four experiments for each individual Rab. Values are expressed as a percentage of the response measured with GST−GDI-2^{WT} in the presence of GDP and represent the mean ± SE.

was performed. This region displays the highest sequence variations vs GDI-1 (*11*), suggesting the possibility that it could provide a mechanism for a distinct Rab-binding specificity between those two isotypes. Similarly to the wild type, the recombinant GST−GDI-$2^{\Delta C18}$ deletion mutant protein, produced in bacterial host and affinity-purified on glutathione−agarose beads, displayed a high level of purity with negligible proteolyzed fragments (Figure 1, lane 4). On SDS−polyacrylamide gels, GST−GDI-$2^{\Delta C18}$ moved slightly faster than GST−GDI-2^{WT}, corresponding to the introduced deletion (Figure 1). The ability of the GST−GDI-$2^{\Delta C18}$ deletion mutant protein to stimulate the release of Rab proteins from the membrane bilayer was assayed relative to GST−GDI-2^{WT}. As demonstrated in Figure 3, the C-terminal truncated mutant demonstrated nearly wild-type activity levels with all of the Rabs examined here, as evident by the

equal or only slightly decreased intensities (up to 30%) of the immunodetected Rab protein bands on the chemiluminescence exposures. As with GDI-2^{WT}, GDP contributed only slightly to the effect observed in its absence, since Rabs are presumably already in their GDP-bound form upon membrane isolation (Figure 3). Similarly to GDI-2^{WT}, the truncated protein was much less effective in Rab retrieval in the presence of GTPγS (Figure 3A, lanes 3 and 6). No immunoreactive Rabs were detected in the soluble fractions of control COS membranes incubated with only GST in the presence of either GDP or GTPγS (data not shown). Together, these findings demonstrate nearly wild-type activity for the GST−GDI-$2^{\Delta C18}$ mutant, indicating that the 18-residue segment of the GDI-2 carboxyl-terminal region neither is substantially involved in direct interaction with Rabs nor serves as a structural scaffold of a GDI-2 Rab-binding domain.

Point Mutations within the GDI-2 Sequence-Conserved Region. Crystallographic studies of GDI-1 revealed that sequence-conserved regions are clustered on one face of the molecule, and mutagenesis confirmed some of the surface residues in this region as candidate Rab-binding amino acids (*26*). The close similarity between the primary sequences of GDI-1 and GDI-2 suggests the possibility that the structural architecture of the GDI-2 Rab-binding region may be similar to that of GDI-1. To begin understanding the role of individual GDI-2 residues in Rab functional binding, we introduced two point mutations within the SCR 3B: Y249V and M250Y. Mutant proteins were produced as GST fusions and were purified to near-homogeneity on glutathione−agarose beads as demonstrated in Figure 1. To determine the effect of the introduced substitutions on the GDI-2 functional property to release Rabs from membranes, the mutant proteins were incubated with isolated and washed COS-7 membranes. In addition, to examine whether the mutants retain the wild-type ability to sense GDP- or GTP-bound conformations of Rabs, aliquots of the membranes were analyzed in the presence of GDP or GTPγS. After incubation, the reactions were pelleted, and the soluble fractions were subjected to immunoblot analysis to determine the content of the Rab proteins. As shown in Figure 4, substitution of Met at position 250 for Tyr resulted in a mutant protein with dramatically abrogated abilities to retrieve all GDP-loaded Rabs examined in this study, including Rab2, Rab4, Rab5, Rab8, Rab9, and Rab11. The slight differences in the extent of inhibition among the individual Rabs were not statistically significant (Figure 4B). Intriguingly, although the activity of GDI-2^{M250Y} was profoundly inhibited, on overexposed films we were able to detect further inhibition in the presence of GTPγS, consistent with the retained property of this mutant of preferentially recognizing the GDP-bound forms of Rabs. When GTPγS substituted for GDP, practically no detectable amounts of solubilized Rabs were documented (Figure 4A,B). These results demonstrate that GDI-2^{M250Y} is largely defective in extracting all of the GDP Rabs examined here and suggest a crucial role of position 250 in the functional GDI-2−Rab interactions.

Surprisingly, substitution of the adjacent residue at position Y^{249} resulted in an unexpected differential effect on the ability to solubilize Rabs. As illustrated in Figure 4A, the ability of GDI-2^{Y249V} was strictly dependent upon Rab

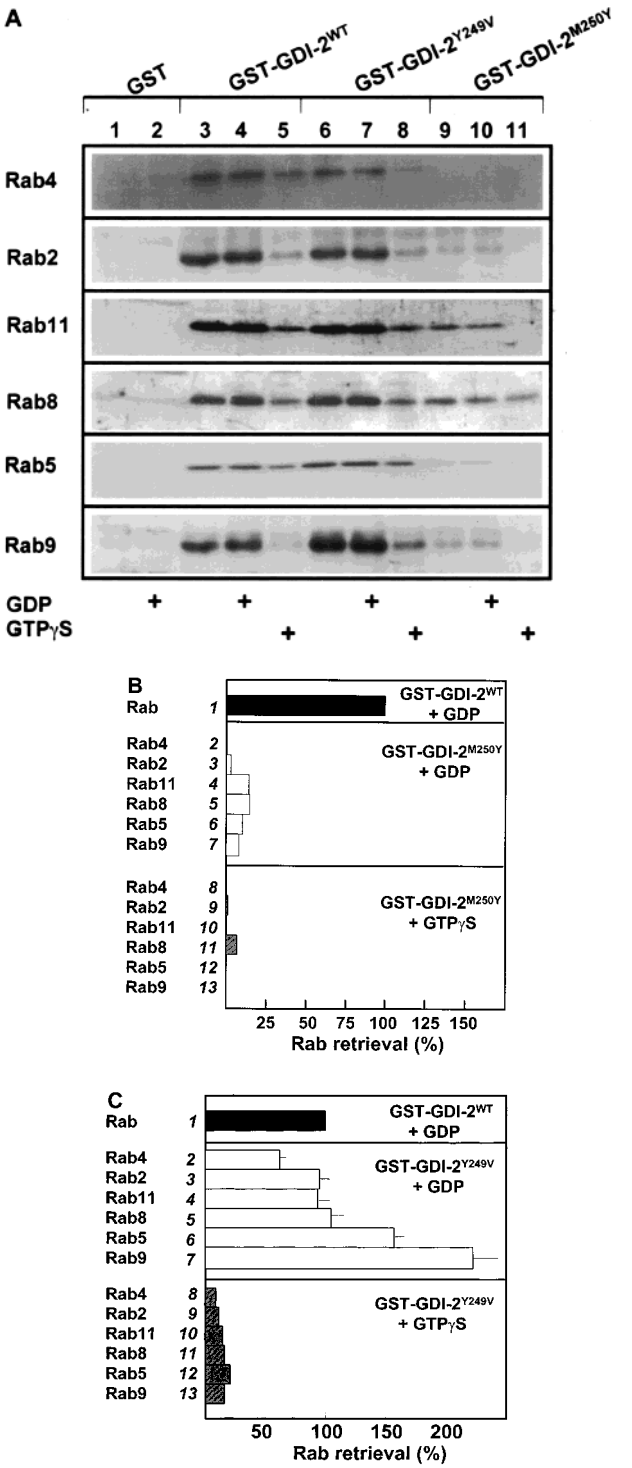

FIGURE 4: Effect of GDI-2 point mutations at positions 249 and 250 on Rab retrieval. Postnuclear membranes isolated from COS-7 cells were preloaded with either GDP or GTPγS (each at 1 mM) for 45 min at 30 °C. Incubations were continued for 30 min at 30 °C in the presence of either GST, GST−GDI-2^{WT}, GST−GDI-2^{Y249V}, or GST−GDI-2^{M250Y} as indicated, each protein at 1 μM. The reaction mixtures were centrifuged, and soluble fractions were analyzed by SDS−PAGE and immunoblotting with the indicated anti-Rab antibodies. Shown are chemiluminescence detections of representative immunoblots (A) and the quantification of densitometric scans (B,C) from three to four independent experiments for each individual Rab. Values are expressed as a percentage of the response measured with GST−GDI-2^{WT} in the presence of GDP and represent the mean ± SE.

protein, and an array of different effects could be observed: a profound to moderate gain-of-function (Rab9 and Rab5),

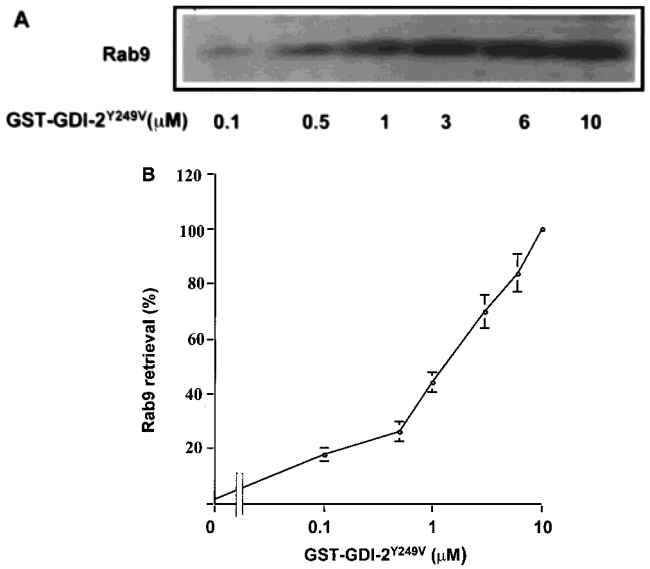

FIGURE 5: Effect of different doses of GST−GDI-2^{Y249V} on Rab9 membrane retrieval. Postnuclear membranes isolated from COS-7 cells were preloaded with GDP (1 mM) for 45 min at 30 °C. Incubation was continued for an additional 30 min at 30 °C in the presence of increasing concentrations of GST−GDI-2^{Y249V} (0−10 μM). The reaction mixtures were centrifuged, and the soluble fractions were analyzed by SDS−PAGE and immunoblotting with anti-Rab9 antibody. (A) Shown is a chemiluminescence detection of a representative immunoblot out of three separate experiments with identical results. (B) Quantification of the densitometric scans expressed as a percentage of the intensity at the highest GST−GDI-2^{Y249V} dose (10 μM) and plotted as a function of the GST−GDI-2^{Y249V} concentration (mean ± SE).

no change (Rab8 and Rab11), and a slight to moderate inhibition (Rab2 and Rab4), as compared to GDI-2^{WT}. Thus, at 1 μM concentration, the activity of GDI-2^{Y249V} to retrieve Rab9 from membranes increased to 220−250% compared to the wild-type activity (Figure 4A,C). Rab5 membrane retrieval was also increased, although to a lesser extent (150% over the wild type) (Figure 4A,C). Conversely, the mutant protein was less effective than the wild-type toward Rab4, and a decrease of ~45% was documented (Figure 4A,C). Importantly, GDI-2^{Y249V} retained the ability to discriminate between GDP- and GTPγS-loaded forms of Rabs (Figure 4A,C). These results demonstrate, first, that substitution at position 249 of GDI-2 yields a gain-of-function conformation and, second, that this conformation markedly discriminates among membrane-bound Rabs, resulting in more than a 5-fold difference in the efficiency of their membrane retrieval.

The increased efficiency of Rab9 retrieval by GDI-2^{Y249V} documented in Figure 4 was observed for all concentrations analyzed here and amounted to a 2−4-fold increase over the wild type. Intriguingly, unlike GDI-2^{WT} (Figure 2), no saturation was achieved even at concentrations as high as 10 μM GDI-2^{Y249V} (Figure 5). Instead, the amounts of retrieved Rab9 were gradually increased with the increase of GDI-2^{Y249V} concentrations (Figure 5), reaching as high as 75% depletion of the total membrane-bound Rab9 (data not shown). These results indicate that the amounts of retrieved Rab9 from membranes could be substantially increased upon substitution of Tyr^{249} in GDI-2.

Tyrosine Phosphorylation of GDI-2 Enhances Its Functional Interactions with Rab4. The observation that GDI-2^{Y249V} exhibits higher capability for functional coupling to specific membrane-bound Rabs than the wild type suggests the possibility that yet to be identified conditions in living cells may induce conformational changes in the GDI-2 molecule, thereby enhancing its functional interactions with Rabs. Our previous studies in 3T3-L1 adipocytes indicated that the endogenous GDI-2, like GDI-1, is not significantly phosphorylated at the basal state, nor is the phosphorylation state modulated upon acute treatment with insulin, known to activate membrane trafficking (*21*, *23*). While one could argue that the optimal conditions to document physiologically relevant GDI phosphorylation in this cell type have not yet been found (*35*), in this study we have exploited the ability of pervanadate, a well-known insulin-mimetic agent (*27*, *36*), to drastically increase phosphotyrosine content in proteins, and particularly that of GDI-2. As we have demonstrated previously, this effect of pervanadate is primarily due to a potent inhibition of the intracellular tyrosine phosphatase activity (*27*). Thus, similarly to the effect in primary rat adipocytes (*27*), a short treatment of 3T3-L1 adipocytes with freshly prepared pervanadate (100 μM) resulted in a profound accumulation of tyrosine-phosphorylated proteins as demonstrated by immunoblotting analysis of total cell lysates with anti-PY antibody 4G10 (data not shown). By immunoprecipitating GDI-2 from these lysates and reprobing the blot consecutively with 4G10 and specific anti-GDI-2 antibodies, we were able to document that GDI-2 is among the tyrosine-phosphorylated proteins under these conditions (Figure 6A, lanes 2 vs 4). To determine whether such posttranslationally modified GDI-2 adopts a conformation which could facilitate interactions with Rabs, we isolated cytosolic GDI-2−Rab4 complexes from pervanadate-treated or control 3T3-L1 adipocyte by immunoprecipitating with anti-Rab4 antibodies, as we described previously (*23*). As a negative control, similar analysis was performed with cytosols of 3T3-L1 adipocytes acutely treated with insulin, which results in an enhanced retrieval of membrane Rab4 in a GDI-2-independent manner, as we have demonstrated previously (*23*) and confirmed here. Thus, as illustrated in Figure 6B−D, similarly to insulin (*23*), pervanadate treatment causes an increase of soluble forms of Rab4, as compared to nontreated cells, which could be readily documented by immunoprecipitating and/or Western blotting of the cytosolic fractions with anti-Rab4 antibodies. Importantly, probing of these Rab4 immunoprecipitates with anti-GDI-2 antibodies revealed significantly higher levels (up to 3-fold) of coprecipitated GDI-2 following pervanadate stimulation of 3T3-L1 adipocytes which correlated with the increased Rab4 levels (Figure 6C−E). Probing with the 4G10 antibody confirmed tyrosine phosphorylation of the coprecipitated GDI-2 from pervanadate-stimulated cells (Figure 6C). By contrast, GDI-1, which failed to accumulate phosphate in its tyrosines at a detectable level upon pervanadate treatment, coprecipitated at levels comparable to control cells (Figure 6C). Consistent with our previously published observations, the level of GDI-2 in Rab4 immunoprecipitates was virtually unaltered upon insulin treatment of these cells, nor was GDI-2 tyrosine-phosphorylated under these conditions (Figure 6C). Similarly, no detectable tyrosine phosphorylation of Rab4 was documented upon

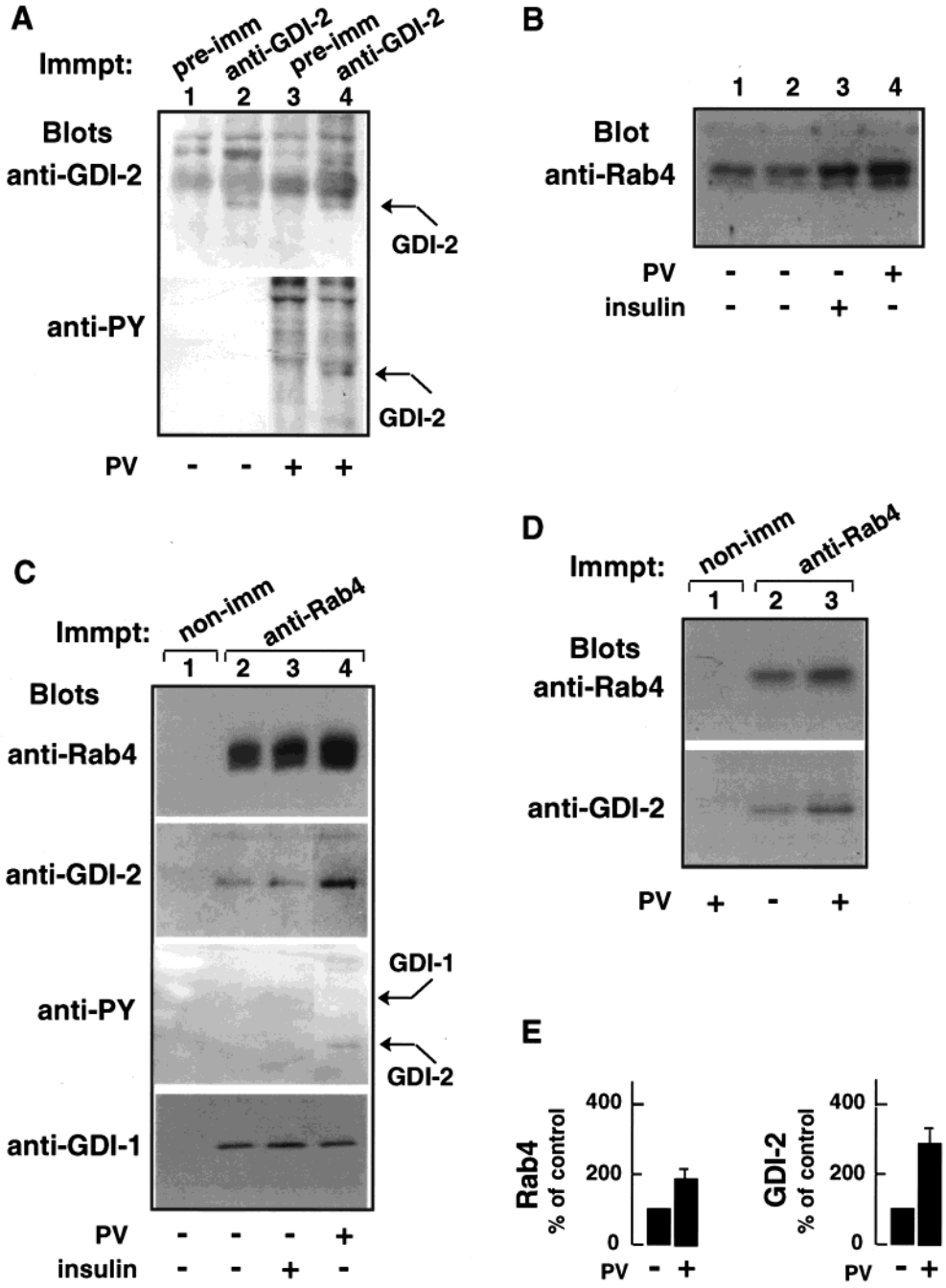

FIGURE 6: Effect of pervanadate treatment of 3T3-L1 adipocytes on GDI-2 tyrosine phosphorylation and Rab4 membrane release. Differentiated 3T3-L1 adipocytes (150 mm dish) were serum-deprived for 3 h and then stimulated for 20 min at 37 °C with pervanadate (100 μM) or insulin (100 nM) as indicated. (A) The cells were lysed in RIPA buffer and immunoprecipitated with anti-GDI-2 (R3362) or preimmune sera as indicated. After washings in RIPA buffer, the proteins were resolved by SDS−PAGE and immunoblotted consecutively with anti-PY antibody (4G10) and anti-GDI-2 IgG (R3361) with a stripping step in between. Shown are chemiluminescence detections of a representative experiment out of two with identical results. (B−D) The cells were homogenized and then fractionated to obtain the cytosol. (B) Cytosolic proteins (70 mg) were analyzed by SDS−PAGE, immunoblotted with polyclonal anti-Rab4 antiserum (1:1000), and detected by chemiluminescence. (C and D) Cytosolic proteins (1.5 mg) were immunoprecipitated (45 min at 4 °C) in the presence of 1 mM GDP with nonimmune IgG or anti-Rab4 IgG cross-liked to protein A−Sepharose Fast Flow. After two washes, GDI proteins associated with Rab4 were eluted with RIPA buffer and analyzed by SDS−PAGE and sequential immunoblotting with anti-PY antibody 4G10, anti-GDI-2 (R3361), or anti-GDI-1 (R3351) IgG with a stripping step in between as indicated. Only GDI-2, but not the GDI-1 band (indicated by arrows), coincides to a tyrosine-phosphorylated protein band. Immunodetection of Rab4 was achieved following its dissociation from the affinity columns by boiling in Laemmli sample buffer, resolution by SDS−PAGE, and immunoblotting with anti-Rab4 antiserum as indicated. Shown are chemiluminescence detections of immunoblots from a representative experiment (C) and an autoradiogram of ^{125}I-protein A-detected immunoblots (D). (E) Quantitation of the blots in panels B and D on the basis of radioactive counting (D) or densitometric scanning (B) of the indicated bands from three independent experiments (in duplicates) with different cytosols (mean ± SE).

either pervanadate or insulin treatment of this cell type (*23*, and data not shown). Together these results indicate, first, that GDI-2 is capable of undergoing tyrosine phosphorylation in living cells and, second, that tyrosine-phosphorylated GDI-2 adopts a conformation exhibiting higher affinity toward Rab4.

DISCUSSION

Recent studies demonstrate that while other proteins besides GDIs could support the initial delivery of nascent Rabs to the appropriate intracellular compartment, Rabs' return to the cytosol could be performed only by GDIs (*32*). Rab GTPases represent a rather diverse group of proteins, differing in structure, intracellular membrane localization, and regulated transport step, yet GDI-1 has been shown to indiscriminately retrieve most, if not all, membrane-bound Rab species (for a review, see ref *8*). The aim of this study was, first, to examine whether the functional ability of GDI-2 to bind and solubilize membrane Rab proteins is restricted to a set of Rabs and, second, to identify structural elements within the GDI-2 molecule that are responsible for Rab functional retrieval. To this end, we have used an in vitro functional assay and tested the activity of GDI-2^{WT} or mutant proteins in modulating the membrane dissociation of various GDP-loaded Rabs exploiting membranes isolated from COS kidney cells, a source especially rich in the Rab species analyzed here. Thus, we have evaluated not only GDI-2 binding to Rabs but also its ability to recognize and access them in the context of a membrane microenvironment of a particular organelle, a system more closely resembling the complexity of membrane interactions in living cells. The members of the Rab family selected for analyses in this study represent prototype markers of different intracellular membrane compartments and transport steps (reviewed in refs *1*−*4*). Thus, Rab4, Rab5, and Rab11 operate in the endocytotic/recycling pathway, being associated with clathrin-coated vesicles and early endosomes (Rab5), endocytic vesicles (Rab4), or perinuclear recycling endosomes (Rab11). Rab9 is found in late endosomes, playing a role in the transport to Golgi. Rab2 and Rab8 support the biosynthetic pathway, and are localized to the ER (Rab2) and the trans Golgi network (Rab8). Despite their quite divergent structure (Table 1), the distinct intracellular membrane localization, and the different transport route of regulation displayed by the Rabs selected here, GDI-2^{WT} appeared to bind and retrieve their GDP-bound forms with similar capacity. In agreement with our data are recent studies demonstrating that the Rab8 and Rab11 differential sensitivity to extraction by GDIs observed in living cells stems from the relative differences in the proportion of their GDP-bound forms (*24*). These results indicate that, similarly to GDI-1^{WT} (*8*, *10*, *11*, *14*, *30*−*33*), GDI-2^{WT} is capable of accessing, recognizing, binding, and solubilizing numerous members of the Rab protein family, as we have predicted in our previous studies (*11*). Thus, despite the characteristic intracellular localization pattern of GDI-2, shown associated with distinct pericentriolar membrane compartments (*21*, *22*), and the possibility for the two isotypes to operate with a distinct subset of Rabs, we found no evidence for any Rab-specific function of GDI-2^{WT} in the in vitro functional assay exploited here. An important conclusion of these experimental data is that GDI-2 may, at least in part, substitute for the absent function of GDI-1. Human studies documented mutations in the *GDI-1* gene in two families affected with X-linked nonspecific mental retardation (*37*). The rather mild phenotype caused by a null mutation in the *GDI-1* gene is consistent with the ubiquitous presence of GDI-2 or GDIβ which can apparently take over the lost function, thus preventing cellular dysfunction throughout the body. That the GDI proteins are critical in coordinating and maintaining accurate intracellular membrane trafficking events is substantiated by the studies demonstrating that an in vivo depletion of the only GDI gene in the budding yeast *S. serevisiae* results in multiple defects in intracellular transport (*38*).

The most significant variations in the amino acid sequence of GDI-1 vs GDI-2/β are concentrated in the C-terminal region. In fact, there are 2 segments of about 18−21 residues, i.e., from amino acid 387 to 403 and from 426 to 447, which display less than 50% homology between the isotypes. These variable regions were initially thought to serve as basis for a Rab-selective interaction of GDI-1 vs GDI-2 (*11*). Moreover, studies in yeast indicate that a temperature-sensitive allele of *S. serevisiae* GDI, *sec 19-1*, which displays a phenotype of severe membrane trafficking disorders, encodes a version of yeast *GDI* differing only by a 17-residue segment C-terminal truncation (*39*). Yeast *GDI* is highly homologous to mammalian GDIs and displays principally similar architecture and function (*38*). Our observation that deletion of the C-terminal 18-residue segment of GDI-2 converts the molecule to nearly fully functional GDI (Figure 3) indicates that a large segment of the C-terminal variable region is excluded from GDI-2 Rab-retrieving elements. Together with the data in yeast *sec 19-1* allele, our results further imply that the variable C-terminal regions of mammalian and yeast GDI are likely engaged in other yet to be determined key interactions necessary for correct intracellular membrane trafficking to occur.

The notion that the variable C-terminal region is excluded from candidate GDI-2 Rab-interacting elements is further supported by the observation that only a single amino acid substitution at position M^{250} within the sequence-conserved regions causes a dramatic decrease in the efficiency of GDI-2^{M250Y} to dissociate all membrane-bound Rabs examined here (Figure 4A,B). This finding agrees with previous mutagenesis studies of GDI-1, where introduction of an identical mutation rendered a GDI-1^{M250Y} mutant incapable of binding Rab3A and Rab1A (*26*, *34*). Together these results indicate Met at position 250 as a common residue in candidate GDI-1 and GDI-2 Rab-binding regions. The fact that substitution at this position still retains the GDI-2^{WT} ability to detect differences between GDP- and GTPγS-bound Rab forms indicates that Met^{250} should be distal to the GDI-2-sensor elements for the GDP load in Rabs.

One unexpected finding made in our study is the observation that certain conformations of the GDI-2 molecule are associated with a gain-of-function in retrieval of specific Rabs. We provide experimental evidence both in vitro and in intact cells for two structural modifications in the GDI-2 molecule which potently convert the relaxed conformation of the wild-type or nonmodified endogenous GDI-2 to a more functionally active conformation, resulting in a more efficient Rab membrane release. The first one is achieved by a single amino acid substitution at position Y^{249} within the sequence-conserved region 3B in GDI-2 (Figure 4A,C). The second modification is induced upon treatment of intact adipocytes with the tyrosine phosphatase inhibitor pervanadate yielding tyrosine-phosphorylated endogenous GDI-2 (Figure 6). While a detailed examination of the issue of GDI-2 tyrosine phosphorylation with respect to an individual tyrosine is beyond the scope of the present study, an important inference

can be drawn, namely, that the tyrosine-phosphorylated GDI-2 adopts a conformation facilitating the in vivo Rab4 membrane retrieval. The molecular basis for the marked and selective enhancement in Rab extraction elicited by these two structural modifications in GDI-2 is presently unknown. However, these observations are consistent with the idea that the resting conformation of GDI-2, and likely GDI-1, is not fully active, and suggest a plausible regulation of GDI activity in the context of intact cells, to modulate spatially and temporally the extent of retrieved Rabs. Moreover, certain discrepancies between the activities of bacterially produced vs native purified GDI-1 are reported (*34*, *40*). It is conceivable that the wild-type GDIs or a pool of endogenous forms in resting cells display limited ability to access, recognize, and/or bind membrane-bound Rabs. This hypothesis is further reinforced by the findings that, typically, 50−60% of the total Rab membrane amounts could be dissociated even at saturating concentrations of GDI-1^{WT} or GDI-2^{WT} as documented in in vitro or semi-intact cell assays (*11*, *26*, *31*, *33*, and this study). Next, an insulin-induced increase of GDI-1-dependent Rab4 membrane retrieval (*23* and this study) also implies regulation of GDI functional activity in living cells. Finally, reports of phosphorylation (*35*) and isoelectric shift of GDIs (*41*) add further support to this hypothesis.

Another important observation made in our study is that a single amino acid replacement in GDI-2 differentially affects Rab membrane retrieval. Thus, while the GDI-2^{Y249V} mutant displayed increased functional activity for Rab9 and Rab5, its efficiency toward Rab4 was significantly compromised (Figure 4). Noteworthy, a recent study, published while this paper was at a final stage of preparation (*34*), has demonstrated that a single amino acid substitution at position 39 within SCR 1 in the GDI-1 molecule yields a mutant protein which also displays distinct effects in Rab3A (inhibition) and Rab1A (no change) retrieval from membranes. Together, these results imply that structural elements of GDI molecules could discriminate the functional interactions with individual Rabs. It is tempting to speculate that in living cells GDIs can undergo subtle organelle-dependent modification(s) that can direct selective interactions with different Rab species, allowing a preferential retrieval and recycling of one Rab over others when they are present together in a given organelle. Our finding that the GDI-2^{Y249V} mutant adopts a conformation that facilitates Rab5 release from endosomal membranes, being less effective toward Rab4, is consistent with this idea. Further insights into this issue should be forthcoming as we learn more about crystal structures of GDI-2 complexed with Rab proteins.

In summary, while GDI-2 displays nearly equal ability to extract GDP bound forms of a diverse group of Rab proteins, substitution of Tyr^{249} differentially modulates Rab membrane retrieval, resulting in a gain-of-function conformation toward specific Rab species. We have identified Met^{250} as being critical for the interactions with all Rabs tested in this study, whereas the C-terminal 18 amino acids were irrelevant. GDI-2 could be tyrosine-phosphorylated in 3T3-L1 adipocytes under certain treatment, a modification that yields a protein with higher Rab4-retrieval activity. We conclude that certain yet to be identified conditions in intact cells may induce conformational changes in the GDI-2 molecule that would facilitate a selective Rab membrane release.

ACKNOWLEDGMENT

We thank Drs. Diego Sbrissa and Ogi Ikonomov for critical reading of the manuscript. The technical help of graduate student Dean Post is highly appreciated. The generous gifts of antibodies from S. Pfeffer, I. Mellman, and M. Zerial are gratefully acknowledged.

REFERENCES

1. Nuoffer, C., and Balch, W. E. (1994) *Annu. Rev. Biochem. 63*, 949−990.
2. Novick, P., and Zerial, M. (1997) *Curr. Opin. Cell Biol. 9*, 196−504.
3. Olkonen, V. M., and Stenmark, H. (1997) *Int. Rev. Cytol. 176*, 1−85.
4. Schimmoller, F., Simon, I., and Pfeffer, S. R. (1998) *J. Biol. Chem. 273*, 22161−22164.
5. Sogaard, M., Katsuko, Y., Ye, R. R., Geromanos, S., Tempst, P., Kirschhausen, T., Rothman, J. E., and Sollner, T. (1994) *Cell 78*, 937−948.
6. Lupashin, V. V., and Waters, M. G. (1997) *Science 276*, 1255−1258.
7. Rybin, V., Ullrich, O., Rubino, M., Alexandrov, K., Simon, I., Seabra, C., Goody, R., and Zerial, M. (1996) *Nature 383*, 266−269.
8. Pfeffer, S., Dirac-Svejstrup, B. A., and Soldati, T. (1995) *J. Biol. Chem. 270*, 17057−17059.
9. Shisheva, A., and Czech, M. (1995) *Guidebook of Small GTPases*, Oxford University Press, Oxford, U.K.
10. Matsui, Y., Kikuchi, A., Araki, S., Hata, Y., Kondo, J., Teranishi, Y., and Takai, Y. (1990) *Mol. Cell. Biol. 10*, 4116−4122.
11. Shisheva, A., Südhof, T. C., and Czech, M. P. (1994) *Mol. Cell. Biol. 14*, 3459−3468.
12. Nishimura, N., Nakamura, H., Takai, Y., and Sano, K. (1994) *J. Biol. Chem. 13*, 14191−14198.
13. Janoueix-Lerosey, I., Jollivet, F., Camonis, J., Marche, P. N., and Goud, B. (1995) *J. Biol. Chem. 270*, 14801−14808.
14. Ullrich, O., Stenmark, H., Alexandrov, K., Huber, L. A., Kaibuchi, K., Sasaki, T., Takai, Y., and Zerial, M. (1993) *J. Biol. Chem. 268*, 18143−18150.
15. Ullrich, O., Horiuchi, H., Bucci, C., and Zerial, M. (1994) *Nature 368*, 157−160.
16. Soldati, T., Shapiro, A. D., Dirac-Svejstup, A. B., and Pfeffer, S. P. (1994) *Nature 369*, 76−78.
17. Dirac-Svejstrup, A. B., Soldati, T., Shapiro, A., and Pfeffer, S. R. (1994) *J. Biol. Chem. 269*, 15427−15430.
18. Horiuchi, H., Giner, A., Hoflack, B., and Zerial, M. (1995) *J. Biol. Chem. 270*, 11257−11262.
19. Dirac-Svejstrup, A. B., Sumizawa, T., and Pfeffer, S. R. (1997) *EMBO J. 16*, 465−472.
20. Chinni, S. R., Brenz, M., and Shisheva, A. (1998) *Exp. Cell Res. 242*, 373−380.
21. Shisheva, A., Buxton, J., and Czech, M. P. (1994) *J. Biol. Chem. 269*, 23865−23868.
22. Shisheva, A., Doxsey, S., Buxton, J., and Czech, M. P. (1995) *Eur. J. Cell Biol. 68*, 143−158.
23. Shisheva, A., and Czech, M. P. (1997) *Biochemistry 36*, 6564−6570.
24. Chen, W., Feng, Y., Chen, D., and Wandinger-Ness, A. (1998) *Mol. Biol. Cell 9*, 3241−3257.
25. Yang, C., Slepnev, V. L., and Goud, B. (1994) *J. Biol. Chem. 269*, 31891−31899.
26. Schalk, I., Zeng, K., Wu, S.-K., Stura, E. A., Matteson, J., Huang, M., Tandon, A., Wilson, I. A., and Balch, W. E. (1996) *Nature 381*, 42−48.
27. Shisheva, A., and Shechter, Y. (1993) *Endocrinology 33*, 1562−1568.
28. Laemmli, U. K. (1970) *Nature 227*, 680−685.
29. Rodbard, D. (1974) *Clin. Chem. 20*, 1255−1270.
30. Beranger, F., Cadwallader, K., Porfiri, E., Powers, S., Evans, T., Gunzburg, J., and Hancock, J. E. (1994) *J. Biol. Chem. 269*, 13637−13643.

31. Peter, F., Nuoffer, C., Pind, S. N., and Balch, W. E. (1994) *J. Cell Biol. 126*, 1393−1406.
32. Wilson, A. L., Erdman, R. A., and Maltese, W. A. (1996) *J. Biol. Chem. 271*, 10932−10940.
33. Raffaniello, R. D., Lin, J., and Raufman, J.-P. (1996) *Biochem. Biophys. Res. Commun. 225*, 232−237.
34. Wu, S.-K., Luan, P., Matteson, J., Zeng, K., Nishimura, N., and Balch, W. E. (1998) *J. Biol. Chem. 273*, 26931−26938.
35. Steele-Mortimer, O., Gruenberg, J., and Clague, M. J. (1993) *FEBS Lett. 329*, 313−318.
36. Shisheva A., Ikonomov, O., and Shechter, Y. (1994) *Endocrinology 134*, 507−511.
37. D'Adamo, P., Menegon, A., Lo Nigro, C., Grasso, M., Gulisano, M., Tamanini, F., Bienvenu, T., Gedeon, A. K., Oostra, B., Wu, S.-K., Tandon, A., Valtorta, F., Balch, W. E., Chelly, J., and Toniolo, D. (1998) *Nat. Genet. 19*, 134−139.
38. Garrett, M. D., Zahner, J. E., Cheney, C. M., and Novick, P. J. (1994) *EMBO J. 13*, 1718−1728.
39. Collins, R. N., Brennwald, P., Garrett, M., Lauring, A., and Novick, P. (1997) *J. Biol. Chem. 272*, 18281−18289.
40. Elazar, Z., Mayer, T., and Rothman, J. E. (1994) *J. Biol. Chem. 269*, 794−797.
41. Zahner, J. E., and Cheney, C. M. (1993) *Mol. Cell. Biol. 13*, 217−221.

BI990200R